

Catalytic reduction of NH_4NO_3 by NO: Effects of solid acids and implications for low temperature DeNO_x processes

Aditya Savara, Mei-Jun Li, Wolfgang M.H. Sachtler, Eric Weitz*

Department of Chemistry and Institute for Catalysis in Energy Processes, Northwestern University,
2145 Sheridan Road, Evanston, IL 60208, United States

Received 9 October 2007; received in revised form 6 December 2007; accepted 12 December 2007
Available online 23 December 2007

Abstract

Ammonium nitrate is thermally stable below 250 °C and could potentially deactivate low temperature NO_x reduction catalysts by blocking active sites. It is shown that NO reduces neat NH_4NO_3 above its 170 °C melting point, while acidic solids catalyze this reaction even at temperatures below 100 °C. NO_2 , a product of the reduction, can dimerize and then dissociate in molten NH_4NO_3 to $\text{NO}^+ + \text{NO}_3^-$, and may be stabilized within the melt as either an adduct or as HNO_2 formed from the hydrolysis of NO^+ or N_2O_4 . The other product of reduction, NH_4NO_2 , readily decomposes at ≤ 100 °C to N_2 and H_2O , the desired end products of DeNO_x catalysis. A mechanism for the acid catalyzed reduction of NH_4NO_3 by NO is proposed, with HNO_3 as an intermediate. These findings indicate that the use of acidic catalysts or promoters in DeNO_x systems could help mitigate catalyst deactivation at low operating temperatures (< 150 °C).

© 2008 Elsevier B.V. All rights reserved.

Keywords: Ammonium nitrate; Ammonium nitrite; NO; NO_2 ; DeNO_x

1. Introduction

Proposals for stricter regulatory standards for diesel exhaust emissions have spurred a flurry of research directed towards efficient low temperature (≤ 150 – 250 °C) NO_x reduction [1,2]. However, NH_4NO_3 , which is thermally stable at < 250 °C [3,4] can form from NH_3 and HNO_3 that is present in DeNO_x gas streams [4–9] and could potentially deactivate low temperature DeNO_x catalysts [5,6]. Reactions which can remove NH_4NO_3 from a DeNO_x stream are therefore of importance.

We have previously shown that the reduction of nitric acid or chemisorbed nitrates by NO can play an important role in low temperature DeNO_x catalysis [7,8]. Based on this result it seemed plausible that NH_4NO_3 could also be reduced by NO to NH_4NO_2 , thereby converting a potential catalyst poison to a desirable DeNO_x intermediate: NH_4NO_2 readily decomposes to $\text{N}_2 + 2\text{H}_2\text{O}$ at ≥ 100 °C, a favorable route for reducing NO_x to N_2 over various DeNO_x catalysts [4,9].

Thermal decomposition of NH_4NO_3 has been studied for many years with some debate about the details of the mechanism

leading to N_2O formation [10–17]. NH_4NO_3 sublimates above 125 °C and undergoes three crystal phase changes [18] between room temperature and its melting point, 170 °C, before decomposing in the melt. If enough water is present (≥ 3 H_2O : NH_4NO_3), NH_4NO_3 dissociates to NH_4^+ and NO_3^- ions [19]. Above ~ 250 °C there is a rapid exothermic decomposition to N_2O and H_2O . This decomposition is accelerated by acids and transition metal cations [12,14,20–23], and decelerated by bases, water, and metal oxides; [12,14,20,22,24] thus changing the effective decomposition temperature. A radical-initiated explosive decomposition to N_2 and H_2O has been reported between ~ 290 and 320 °C [12,14,16,25]. For these reasons we have limited our study to $\leq \sim 250$ °C.

Though previous publications do not report that NO reduces NH_4NO_3 below its melting point of 170 °C [6–8], the present study shows that acids do catalyze this reaction below 170 °C.

2. Experimental

2.1. Materials

Na-Y Zeolite powder, $> 90\%$ –100 mesh (< 149 μm), nominal Si/Al = 2.5, was obtained from Aldrich (#33,444-8). BaNa-Y

* Corresponding author. Tel.: +1 847 491 5583; fax: +1 847 491 7713.

E-mail address: weitz@northwestern.edu (E. Weitz).

was prepared from the Na-Y zeolite stock by ion exchange in a 0.1 M $\text{Ba}(\text{NO}_3)_2$ aqueous solution at room temperature. The mixture was stirred for >24 h, then vacuum filtered with a deionized water, washed and then dried. Elemental analysis by inductively coupled plasma spectroscopy (ICP) yielded a zeolite framework composition of $\text{Ba}_{9.6}\text{Na}_{33.8}\text{Al}_{53}\text{Si}_{139}\text{O}_{384}$.

H-Y zeolite samples were prepared by baking $\text{NH}_4\text{-Y}$ in air at 400 °C for >3 h. $\text{NH}_4\text{-Y}$ was obtained from Zeolyst International (# CBU 712), with a nominal Si/Al ratio of 6. An actual Si/Al of 3.76 ± 0.45 was determined by ICP.

The quartz used in these studies was Davison Grade # 62, 80–200 mesh (74–177 μm) which was washed with 1 M HNO_3 , and baked at 400 °C for 3 h. Trimethylated quartz was prepared by stirring the 74–177 μm quartz crystals in >98% chlorotrimethylsilane, obtained from Lancaster Synthesis (# 200-900-5). A second sample of smaller quartz crystals, –325 mesh (<44 μm) 99.6% SiO_2 was used as obtained from Aldrich (#34,289-0).

NH_4NO_3 was obtained from Aldrich (#22,124-4, >98% purity). The water content/purity of the NH_4NO_3 was checked by titration with NaOH in water. A glass electrode pH probe was used during titration, with the equivalence point observed at a pH of ~10.3 as determined by the point of maximum change in pH per volume of titrant. A resolution of 0.1 pH units was required to observe the equivalence point. The quantity of NaOH required for titration corresponded to NH_4NO_3 samples being $102.2 \pm 2.5\%$ NH_4NO_3 by weight—in excess of the expected quantity of NaOH required for titration. For the three samples that were used in the titrations, values >101.3% were found. Though this is within experimental error of 100%, an “excess” of NaOH required during titration could be explained as resulting from a loss of NH_3 to the gas phase, leaving “excess” HNO_3 behind. This type of behavior has previously been observed with $\text{NH}_4\text{NO}_3(l)$ (>170 °C) and for $\text{NH}_4\text{NO}_3(s)$ at >100 °C [26,27]. In either case, there was no significant quantity of water present in the NH_4NO_3 .

He and 2% NO in He was used as obtained from Matheson Tri-Gas.

2.2. Experimental setup and sample preparation

NH_4NO_3 was ground in a ceramic mortar and pestle prior to mixing with other solids, as it was deemed desirable that in all experiments the NH_4NO_3 particles have the same size. Note: very small quantities of ammonium nitrate were ground at any one time to minimize the scale of a possible decomposition reaction initiated by grinding. Optical microscopy showed that grinding NH_4NO_3 mixed with other powders resulted in smaller NH_4NO_3 crystals than grinding NH_4NO_3 by itself; presumably due to a ball milling effect [28,29].

In flow experiments, samples of ground NH_4NO_3 powder (0.2 g) were used “as is” or physically mixed with another powder (0.07 g) and placed in a quartz U-shaped reactor. The amount of NH_4NO_3 was in excess of the total moles of NO flowed during the duration of an experiment. Either He or NO in He was allowed to flow first through the reactor and then through a quartz cell that was sealed with NaCl windows. The gas in the flow was

monitored by FTIR using a Thermo Nicolet Nexus 670 FTIR spectrometer. The IR beam passed through the chamber surrounding the IR flow-through cell, which was continuously purged with dry air to lessen background fluctuations. IR spectra were obtained at a resolution of 2 or 4 cm^{-1} , by averaging >8 scans taken over ~1 min. Backgrounds were obtained before an experiment by averaging ≥ 20 scans with a 10 cc/min He flow at atmospheric pressure. During experiments, samples were exposed to a 2% NO in He flow of 10 cc/min, with a temperature ramp of 5 °C/min from 25 to 250 °C.

Experiments in which NH_4NO_3 melts were exposed to $^{15}\text{NO}_2$ were performed in a quartz U-tube reactor (surrounded by a cylindrical heating jacket) which was connected to a glass bulb filled with NO_2 . This U-tube reactor was also separated by a valve from a static FTIR cell described elsewhere [30]. The FTIR cell was evacuated, and aliquots were drawn from the gas phase of the U-reactor subsequent to cooling of the NH_4NO_3 melt. FTIR scans were taken at 2 or 4 cm^{-1} resolution, with >4 scans averaged per spectrum. Backgrounds were obtained with ≥ 8 scans.

3. Results

3.1. Reduction of NH_4NO_3 in a flow of NO

NO was allowed to flow over NH_4NO_3 that was physically mixed with different solids; the effluent monitored by IR. Figs. 1 and 2 show the depletion of NO in the effluent as a function of temperature; this consumption of NO is indicative of the reduction of NH_4NO_3 by NO. Fig. 1 shows the depletion of NO for NH_4NO_3 physically mixed with solids containing varying amounts of hydroxyl groups, while Fig. 2 shows the depletion of NO for NH_4NO_3 physically mixed with solids of varying acidities. Production of NO_2 , N_2O_4 , N_2O_3 , HNO_3 , H_2O and N_2O was also observed in the effluent. For all samples, N_2O production from the thermal decomposition of NH_4NO_3 was typically observed between 200 and 250 °C; this production is rapid between 230 and 250 °C. The N_2O_3 observed is expected to arise from the equilibrium with $\text{NO} + \text{NO}_2$.

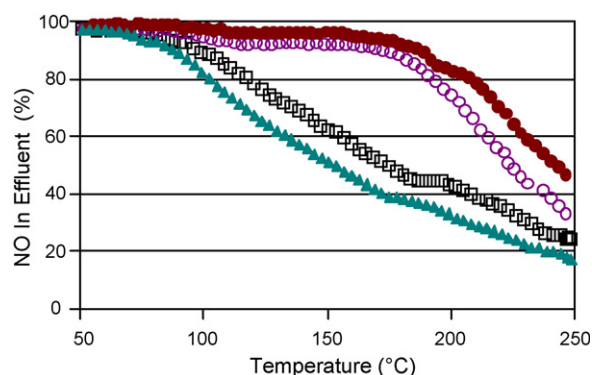


Fig. 1. NO depletion during temperature programmed reaction of neat NH_4NO_3 and NH_4NO_3 physically mixed with solids with varying amounts of surface hydroxyl groups. From top to bottom, NH_4NO_3 —no substrate (filled circles), trimethylated 74–177 μm quartz (open circles), 74–177 μm quartz (open squares), and <44 μm quartz (filled triangles).

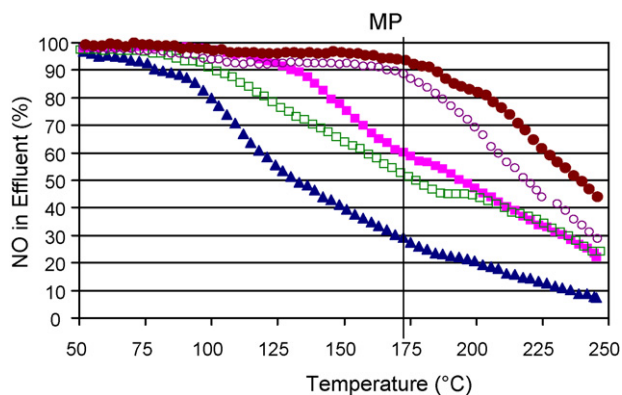


Fig. 2. NO depletion during temperature programmed reaction of neat NH_4NO_3 and NH_4NO_3 physically mixed with four different solids: NH_4NO_3 —no substrate (filled circles), trimethylated quartz (open circles), Na-Y zeolite (filled squares), quartz (open squares), H-Y (filled triangles). Results for BaNa-Y (not shown) were qualitatively and quantitatively similar to Na-Y. For comparison the melting point of NH_4NO_3 (MP) is marked with a vertical line.

Concentration profiles for NO_2 were not stoichiometrically commensurate with NO depletion: less NO_2 production was observed in the effluent than the amount of NO depleted. As shown in Fig. 3, during cooling of the melt to a temperature near the 170 °C freezing point of NH_4NO_3 , a “release” of NO_2 to the gas phase was observed. The amount of NO_2 released in such a manner varied between samples. H-Y mixtures showed the least NO_2 in the effluent during heating and the greatest amount of NO_2 released during cool down.

3.2. Static experiments: exchange of labeled NO_2

To gain insight into the ability of molten NH_4NO_3 to “trap” NO_2 and release NO_2 upon freezing, NH_4NO_3 powder was exposed to $^{15}\text{NO}_2$. Heating of this sample to 200–250 °C (above the melting point of NH_4NO_3) was followed by cooling. Aliquots of the gas were then analyzed to determine whether isotopic exchange occurred between $^{15}\text{NO}_2$ and molten NH_4NO_3 . Isotopic exchange has mechanistic implications which will be discussed below.

The $^{15}\text{NO}_2/\text{NH}_4\text{NO}_3$ mole ratio was varied between 0.01 and 1.0. Based on a lack of NO_2 depletion in the gas phase, and the

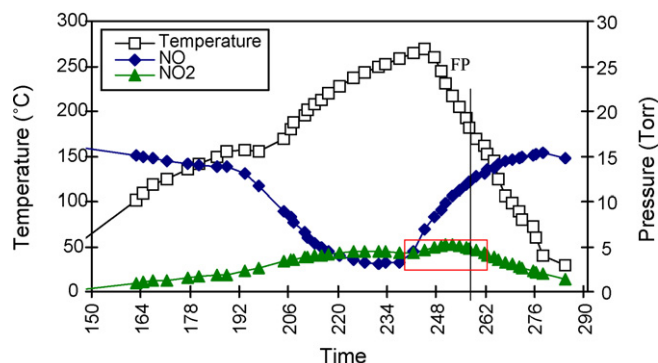


Fig. 3. NO_2 and NO concentrations observed in the effluent as a function of time during heating and cooling, for a flow experiment with NH_4NO_3 physically mixed with quartz and exposed to NO. The freezing point temperature is marked by “FP” and NO_2 released near the freezing point is highlighted by a box.

finite NO_2 isotopic exchange observed in aliquots, molten NH_4NO_3 only accommodates NO_2 as $\ll 3\%$ of the melt. Small quantities of gas phase water and N_2O were also observed after each treatment, presumably the result of the thermal decomposition of a small amount of NH_4NO_3 .

4. Discussion

4.1. Effect of mixing with solid powders

While previous publications show that NO reduces NH_4NO_3 [6–8] above its melting point of 170 °C [15], the data in Figs. 1 and 2 show that when crystalline NH_4NO_3 is physically mixed with some solids, it is reduced by NO *even at temperatures significantly below its melting point*.

The effects of mixing micron-scale particles of NH_4NO_3 with micron-scale particles of other powders can be rationalized when considering the mobility of NH_4NO_3 at the operative temperatures. The temperature at which reaction is observed is above the Hüttig and Tamman temperatures for NH_4NO_3 . These are the temperatures at which mobility of the solid develops at the *surface* ($\sim 1/3$ of the melting point in K) or within the *bulk* ($\sim 1/2$ of the melting point in K), respectively [31]. At these temperatures, the mobility of NH_4NO_3 allows it to spread over the surface of a solid powder. In the case of zeolites, it has previously been shown that molten NH_4NO_3 also enters Faujasite pores [32,33].

By coating the inner and/or outer surfaces of the solids, the NH_4NO_3 acquires an increased surface area and intimate contact with the solid’s surface sites. The promotion of a reaction due to physically mixing NH_4NO_3 with solids could thus be due to either (a) the increased surface area of NH_4NO_3 —a physical effect, or (b) interaction of NH_4NO_3 molecules with the terminations of the surfaces of the solids—a chemical effect.

Quartz surfaces expose weakly acidic hydroxyl groups ($>90\%$ of terminations) [34,35]. To ascertain whether the effect of solid powders on the reduction of NH_4NO_3 by NO is physical or chemical in nature, we compared three quartz samples: 74–177 μm quartz crystals, 74–177 μm quartz crystals passivated by trimethylsilane chloride, and $<44 \mu\text{m}$ quartz crystals. The treatment of the 74–177 μm quartz crystals with trimethylsilane converts hydroxyl groups to trimethylsilanes, dramatically altering the chemical nature of the surface without changing the surface area or volume of the particles. Conversely, the $<44 \mu\text{m}$ quartz crystals exposes more hydroxyl groups per unit of mass than the 74–177 μm quartz crystals due to a larger surface area. The results in Fig. 1 show a clear correlation between the quantity of hydroxyl groups and the promotion of the reduction of NH_4NO_3 by NO. Note that the trimethylsilated quartz has virtually no effect in promoting the reaction. These results indicate that the effect of mixing with solid powders is chemical.

As shown in Fig. 2, there is also a positive correlation between the acidity of a solid and its effect on the reduction of NH_4NO_3 . The extent of reaction is correlated with the acidity of the solids as measured [36–38] by the heat of adsorption for NH_3 : H-Y ($\sim 110 \text{ kJ}$) [39,40] $>$ quartz ($\sim 70 \text{ kJ}$) [41,42] $>$ Na-Y

(~60 kJ)[43] > trimethyl-silated quartz [44]—implying that the reduction of NH_4NO_3 by NO is acid catalyzed. Results for BaNa-Y (not shown in Fig. 2) were qualitatively and quantitatively similar to Na-Y. This is not unexpected since it seems reasonable that these two zeolites would have similar acidities. Note that to our knowledge the heat of adsorption for ammonia on trimethylsilane has not been measured. However, based on data in the literature the heat of adsorption for ammonia on a surface covered with methyl groups is expected to be negligible [44].

4.2. Mechanism

Previous studies have shown that NH_4NO_3 is reduced by NO above 170 °C [6–8]. NH_4NO_3 melts at 170 °C [15] and is in equilibrium with HNO_3 and NH_3 within the melt: [15,45]



As was alluded to in Section 1, NO can reduce HNO_3 to HNO_2 and $\text{NO}_{3(\text{ads})}^-$ to $\text{NO}_{2(\text{ads})}^-$ [8] at or below 40 °C [46]. The fact that neat NH_4NO_3 is reduced by NO only above its melting point (where Eq. (1) is valid) suggests that NH_4NO_3 first dissociates to HNO_3 , and that HNO_3 is subsequently reduced by NO to HNO_2 . Similar interpretations have been presented by others [6,7,47].

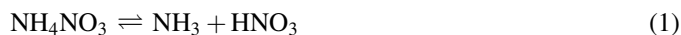
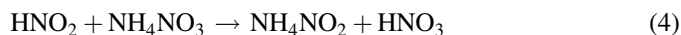
The role of acid sites may then be to reversibly bind NH_3 , thereby making HNO_3 available for reduction to HNO_2 by NO. Reversible binding of NH_3 by silanols has also previously been credited with increasing the efficiency of NO_x reduction by NH_3 [48]. Subsequent to reduction, HNO_2 can recombine with either its geminal NH_3 —thereby regenerating the acid site onto which the NH_3 molecule was adsorbed; or it can combine with the NH_3 of another NH_4NO_3 molecule, thus freeing up another HNO_3 . The sets of steps in this sequence of reactions are then:



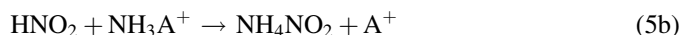
The first steps in the mechanism produce HNO_3 with the binding of NH_3 by the acid, A^+ , through either (2b), or (1 + 2a). HNO_3 is a crucial intermediate that can be reduced by NO to HNO_2 :



If HNO_2 combines with NH_3 from another NH_4NO_3 molecule through either (5a + 1) or (4):



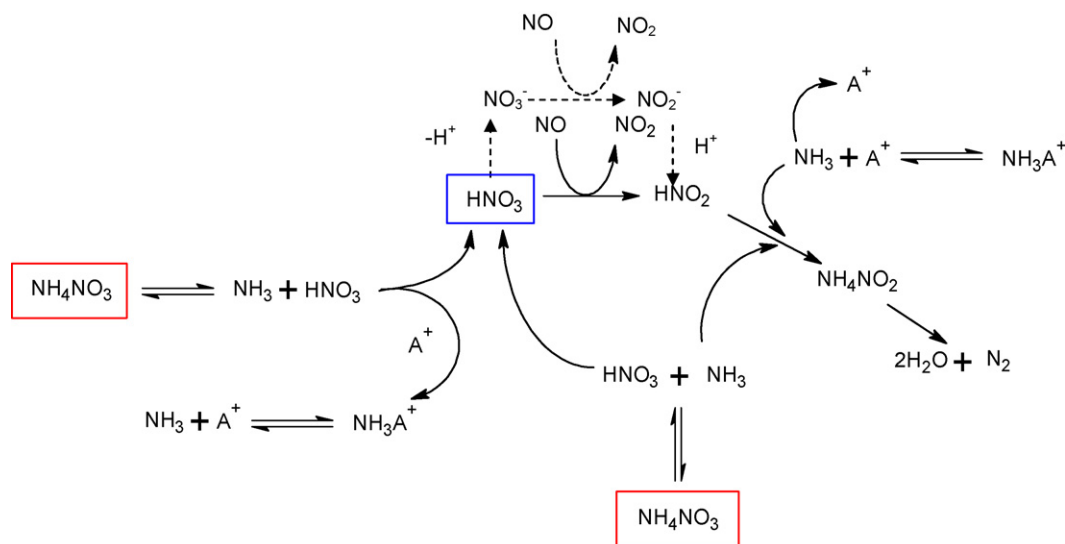
an HNO_3 is produced and this cycle returns to (3). Alternatively, if HNO_2 combines with an NH_3 molecule that was bound to an acid site



through either (5b) or (2a + 5a), then the acid site, A^+ , is regenerated and the cycle involving acidic sites can restart at (2a) and (2b). Subsequent to either cycle, NH_4NO_2 decomposes to yield the desired products:



The proposed mechanism is shown in Scheme 1, with the route involving chemisorbed nitrates indicated by dashed arrows and Eqs. (2b) and (5b) omitted for clarity. Note that there are two cycles. In the first of the two cycles, HNO_2 acquires an NH_3 partner from an NH_4NO_3 molecule (4) or (5a + 1), and an HNO_3 molecule is produced, returning the mechanism to (3). Alternatively, if HNO_2 acquires an NH_3 partner from an acid site (2a + 5a) or (5b), then A^+ is regenerated, and this cycle returns the mechanism to (1 + 2a) or (2b). In addition to the reactions listed above, on some surfaces (such as cationic sites



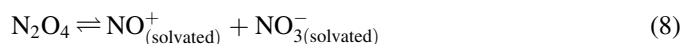
Scheme 1. Proposed mechanism for the acid catalyzed reduction of NH_4NO_3 by NO.

of Na-Y and BaNa-Y) HNO_3 can dissociate and form chemisorbed surface nitrates [30,49], which can then be reduced by NO [8].

This proposed mechanism allows for the first cycle, which does not require acid sites once initiated (Eqs. (1) and (3)–(5)), to continue within the bulk of the NH_4NO_3 melt or on other portions of the mixture's surfaces (i.e., away from the catalytic sites). Consistent with our result that the catalysis of the reduction of NH_4NO_3 by NO is positively correlated with a solids NH_3 adsorption enthalpy, the mechanism also implies that both Brønsted and Lewis acids should catalyze the reduction of NH_4NO_3 by NO.

4.3. NO_2 sequestration and exchange

The flow experiments on the reduction of NH_4NO_3 by NO show that NO_2 is released from the melt during cooling down at approximately the temperature of crystallization of the samples (Fig. 3). One possible explanation is that NO_2 dimerizes to N_2O_4 which then dissociates heterolytically within the NH_4NO_3 melt as shown below:



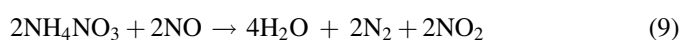
Upon freezing, the reverse reaction in Eq. (8) will be favored if the melt is a more favorable environment for ion solvation than the crystalline solid. The reactions in Eq. (8) are known to occur in highly polar environments such as Faujasite channels, [8,30,49,50] $\text{HNO}_3(l)$ [51] and other polar solutions [51]. It is also known that NH_4NO_3 solvates nitrate salts [52], is soluble in $\text{HNO}_3(l)$, [53] and exists in dissociative equilibrium (1) with $\text{HNO}_3(l)$ when molten [15,45]. This supports the concept that molten NH_4NO_3 might also solvate $\text{NO}_3^- + \text{NO}^+$ as in equation (8).

When molten NH_4NO_3 is exposed to $^{15}\text{NO}_2$ and cooled until it solidifies, both $^{14}\text{NO}_2$ and $^{15}\text{NO}_2$ are observed in the gas phase. Based on Eqs. (7) and (8), some of the observed NO_2 is due to dissociation of N_2O_4 (7) which is “stored” in the melt as NO_3^- and NO^+ (8). The ions in the melt produced from $^{15}\text{NO}_2$ through Eqs. (7) and (8) are expected to be labeled: $^{15}\text{NO}^+$ and $^{15}\text{NO}_3^-$. Since $^{15}\text{NO}_3^-$ is expected to exchange with an unlabelled nitrate from the melt while $^{15}\text{NO}^+$ would not be expected to exchange, partial isotopic exchange would be expected, as was observed.

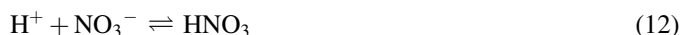
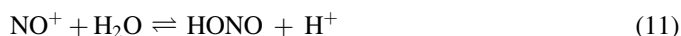
However, the NH_4NO_3 melt (above 170 °C) was only observed to trap $\ll 0.03$ (3 mol%) NO_2 molecule per NH_4NO_3 molecule. It is unclear if the inability of NH_4NO_3 to retain larger quantities of NO_2 in these static experiments, is due to experimental conditions (e.g., extent of evacuation, lack of gas flow, lack of mixing, etc.), or other causes such as the absence of added NO. As a comparison $\text{HNO}_3(l)$ accommodates 10.2 mol% N_2O_4 (in equilibrium with NO^+ and NO_3^- with the equilibrium heavily shifted toward these products) when calculated based on the total number of moles in the melt near room temperature [51], or 18.5 mol% NO_2 , based on the number of NO_2 molecules stored.

For static cell experiments, where $\text{NH}_4\text{NO}_3(l)$ is only exposed to NO_2 , such quantities of dissolved NO_2 ($\ll 3$ mol%) are too low to rationalize the levels of dissolved NO_2 observed during flow experiments in which molten NH_4NO_3 is exposed to NO: in some of these latter experiments the stored NO_2 corresponded to >10 mol% of the melt. An alternative explanation for the apparent sequestration and subsequent release of NO_2 during flow experiments is that during reduction of NH_4NO_3 by NO an intermediate is formed from NO_2 , and this intermediate is stabilized within the melt, released upon freezing, and decomposes to produce NO_2 .

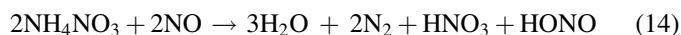
HNO_2 (HONO) is one possible candidate for an intermediate formed from NO_2 and stabilized within the melt until freezing. During the reduction of NH_4NO_3 by NO, NO_2 is first produced before being stored in the melt until cool down:



If the hydrolysis of NO^+ can occur in the NH_4NO_3 melt, HNO_2 will be produced (11). This hydrolysis is known to occur when a salt containing NO^+ as a cation is dissolved in water [54] and is also believed to occur on BaNa-Y [8]. If (11) can occur in the NH_4NO_3 melt, then:



where (13) is the sum of Eqs. (10)–(12). Even if (11) is not significant in the melt, other mechanisms that produce HONO as in (13), may take place, such as through $\text{N}_2\text{O}_4 + \text{H}_2\text{O}$ [55]. Adding (9 + 13) yields:



Reaction (14) would create an excess of acids over ammonia within the melt $[\text{HNO}_3] + [\text{HONO}] > [\text{NH}_3]$. The excess HNO_3 in the melt created from NO_2 and H_2O (13) would catalyze reaction 1 as described in Section 4.2. It is possible that the HONO formed is an intermediate stabilized by the melt. Upon cool down, HNO_2 likely cannot be stabilized within the NH_4NO_3 crystal, and decomposes to NO_2 and H_2O by the reverse of (13) along with the excess HNO_3 . Such a mechanism can explain the stored NO_2 observed during flow experiments. Another implication of reactions (9)–(13) is that the production of water from the reduction of NH_4NO_3 by NO will catalyze the reduction of NH_4NO_3 by NO, as a result of the production of more nitric acid within the melt. While this is one possible explanation for the storage and release of NO_2 , other explanations are also possible, such as an NO_2 adduct stabilized within the melt.

4.4. Generality of the proposed mechanism

The mechanism proposed in Section 4.2 for the acid catalyzed reduction of NH_4NO_3 by NO is likely to be applicable

to other systems. Nova et al. have shown that the catalyzed reduction of NH_4NO_3 by NO on VO_x sites proceeds by a redox mechanism above the melting point of NH_4NO_3 , and that WO_x sites do not catalyze this reaction [6,47,56,57]. A number of factors could explain why some acidic materials do not follow the mechanism proposed in Section 4.2:

- (1) The material binds HNO_3 or HNO_2 too strongly.
- (2) The material binds HNO_3 either molecularly or dissociatively in a manner where HNO_3 can no longer be efficiently reduced by NO.
- (3) If Eq. (4) is not significant, then below 170 °C the geminal NH_3 must be released from the acid site for NH_4NO_2 to be produced, in which case acid sites that bind NH_3 too strongly would not follow our mechanism below 170 °C.

4.5. Implications for low temperature NO_x abatement

The melting point of NH_4NO_3 , ~ 170 °C, has been shown to be a critical temperature below which some DeNO_x catalysts are known to deactivate [5,6], possibly because NO does not efficiently reduce pure NH_4NO_3 below 170 °C [6,7] in the absence of acid sites. The presence of acidic sites, on the catalyst or on added promoters, in low temperature DeNO_x catalysts could potentially lower this critical deactivation temperature to < 100 °C. These sites enhance the production of HNO_3 , which is reduced by NO at temperatures as low as 25 °C [46]. Thus, it may be possible for acids to catalyze the reduction of NH_4NO_3 by NO at temperatures as low as 25 °C.

The product of the reduction of NH_4NO_3 by NO is NH_4NO_2 , a desirable intermediate for low temperature NO_x reduction, since it decomposes to N_2 and H_2O at ~ 100 °C. In prior work, we have demonstrated that in the presence of strong acids NH_4NO_2 decomposes to N_2 and H_2O at temperatures as low as 25 °C [58]. In combination, these findings suggest that incorporating acidic promoters in DeNO_x catalysts, could lower the operational temperatures of DeNO_x systems.

5. Conclusions

NH_4NO_3 is reduced by NO above its melting point, 170 °C. In the presence of acidic solids this reaction is catalyzed and becomes observable at temperatures as low as 70 °C. Based on the proposed mechanism, it is possible that the acid catalyzed reduction could take place at temperatures as low as 25 °C. HNO_3 is a crucial intermediate in the reduction of ammonium nitrate. The reduction product is NH_4NO_2 , a desirable intermediate in low temperature DeNO_x catalysis as it decomposes cleanly to N_2 and H_2O at 100 °C, and at lower temperatures in an acidic environment. Molten NH_4NO_3 may stabilize $\text{NO}_3^- + \text{NO}^+$ that is formed by the heterolytic dissociative solvation of N_2O_4 , which in turn results from the dimerization of NO_2 (Eqs. (7) and (8)). In addition, an intermediate formed from NO_2 is likely stabilized within the melt: one possibility is HNO_2 formed from the hydrolysis of NO^+ or N_2O_4 (10)–(13). When the melt freezes, the reverse of these reactions leads to the rapid release of NO_2 .

These findings suggest that acidic catalysts could lower the effective temperatures for DeNO_x systems by catalyzing the reduction of NH_4NO_3 , a potential deactivator of the catalyst, to NH_4NO_2 , a desirable intermediate in low temperature DeNO_x catalysis.

Acknowledgements

This work was supported by the Chemical Sciences, Geosciences and Biosciences Division, Office of Basic Energy Sciences, Office of Science, U.S. Department of Energy (DE-FG02-03-ER15457), at the Northwestern University Institute for Catalysis in Energy Processes. We would like to thank one of the reviewers for pointing out the possibility of the hydrolysis of NO^+ which is now discussed in Sections 4.1 and 4.3. A. Savara thanks Danielle Gray for useful discussions at a BIP seminar at Northwestern.

References

- [1] F. Klingstedt, K. Arve, K. Eranen, D.Y. Murzin, *Acc. Chem. Res.* 39 (2006) 273–282.
- [2] M.V. Twigg, *Appl. Catal. B* 70 (2007) 2–15.
- [3] H.L. Saunders, *J. Chem. Soc., Trans.* 121 (1922) 698.
- [4] M.J. Li, J. Henao, Y. Yeom, E. Weitz, W.M.H. Sachtler, *Catal. Lett.* 98 (2004) 5–9.
- [5] M. Koebel, M. Elsener, G. Madia, *Ind. Eng. Chem. Res.* 40 (2001) 52–59.
- [6] C. Ciardelli, I. Nova, E. Tronconi, D. Chatterjee, B. Bandl-Konrad, *Chem. Commun.* (2004) 2718–2719.
- [7] M. Koebel, G. Madia, M. Elsener, *Catal. Today* 73 (2002) 239–247.
- [8] Y.H. Yeom, J. Henao, M.J. Li, W.M.H. Sachtler, E. Weitz, *J. Catal.* 231 (2005) 181–193.
- [9] I. Nova, C. Ciardelli, E. Tronconi, D. Chatterjee, M. Weibel, *Top. Catal.* 42/43 (2007) 43–46.
- [10] J.H. MacNeil, H.T. Zhang, P. Berseth, W.C. Trogler, *J. Am. Chem. Soc.* 119 (1997) 9738–9744.
- [11] D.G. Patil, S.R. Jain, T.B. Brill, *Propellants, Explosives, Pyrotechnics* 17 (1992) 99–105.
- [12] K.R. Brower, J.C. Oxley, M. Tewari, *J. Phys. Chem.* 93 (1989) 4029–4033.
- [13] Z.G. Szabo, E. Hollos, J. Trompler, *Zeitschrift fuer Physikalische Chemie* 144 (1985) 187–193.
- [14] J.C. Oxley, J.L. Smith, E. Rogers, M. Yu, *Thermochim. Acta* 384 (2002) 23–45.
- [15] W.A. Rosser, S.H. Inami, H. Wise, *J. Phys. Chem.* 67 (1963) 1753.
- [16] K.J. Kim, C.-S. Lee, W.Y. Lee, *Hwahak Konghak* 11 (1973) 30–36.
- [17] S.K. Adhya, S.K. Mukherjee, B.K. Banerjee, *J. Indian Chem. Soc.* 57 (1980) 321–324.
- [18] R.N. Brown, A.C. McLaren, *Proc. R. Soc. Lond., Ser. A* 266 (1962) 329.
- [19] P.A.M. Walker, D.G. Lawrence, G.W. Neilson, J. Cooper, *J. Chem. Soc., Faraday Trans. I* 85 (1989) 1365–1372.
- [20] J.C. Oxley, S.M. Kaushik, N.S. Gilson, *Thermochim. Acta* 212 (1992) 77–85.
- [21] E.B. Moshkovich, I.I. Strizhevsky, L.I. Kosinova, V.I. Tumanova, *Khimicheskaya Promyshlennost* (1983) 670–672.
- [22] G.-l. Wang, X.-c. Xu, *J. Zhengzhou Univ.* 24 (2003) 47–50.
- [23] S. Skaribas, T.C. Vaimakis, P.J. Pomonis, *Thermochim. Acta* 158 (1990) 235–246.
- [24] A. Kolaczowski, A. Biskupski, A. Lisowski, *Chemia Stosowana* 20 (1976) 311–326.
- [25] H.J. Heinrich, *Explosivstoffe* 12 (1964) 23–27.
- [26] Y.I. Rubtsov, A.I. Kazakov, D.B. Lempert, G.B. Manelis, *Russ. J. Appl. Chem.* 77 (2004) 1083–1091.
- [27] M. Olszak-Humienik, *Thermochim. Acta* 378 (2001) 107–112.

- [28] L.G. Austin, R.R. Klimpel, P.T. Luckie, *Process Engineering of Size Reduction: Ball Milling*, Society of Mining Engineers of the AIME, New York, N.Y., 1984.
- [29] M.W. Gao, E. Forssberg, *Powder Technol.* 84 (1995) 101–106.
- [30] Y.H. Yeom, B. Wen, W.M.H. Sachtler, E. Weitz, *J. Phys. Chem. B* 108 (2004) 5386–5404.
- [31] A.S.J. Baker, A.S.C. Brown, M.A. Edwards, J.S.J. Hargreaves, C.J. Kiely, A. Meagher, Q.A. Pankhurst, *J. Mater. Chem.* 10 (2000) 761–766.
- [32] M. Park, S.C. Shin, C.L. Choi, D.H. Lee, W.T. Lim, S. Komarneni, M.C. Kim, J. Choi, N.H. Heo, *Microporous Mesoporous Mater.* 50 (2001) 91–99.
- [33] A. Carvalho, J. Pires, P. Veloso, M. Machado, M.B. de Carvalho, J. Rocha, *Microporous Mesoporous Mater.* 58 (2003) 163–173.
- [34] M.V. Koudriachova, J.V.L. Beckers, S.W. de Leeuw, *Comput. Mater. Sci.* 20 (2001) 381–386.
- [35] Y. Duval, J.A. Mielczarski, O.S. Pokrovsky, E. Mielczarski, J.J. Ehrhardt, *J. Phys. Chem. B* 106 (2002) 2937–2945.
- [36] H.G. Karge, V. Dondur, *J. Phys. Chem.* 94 (1990) 765–772.
- [37] H.G. Karge, V. Dondur, J. Weitkamp, *J. Phys. Chem.* 95 (1991) 283–288.
- [38] W.E. Farneth, R.J. Gorte, *Chem. Rev.* 95 (1995) 615–635.
- [39] K. Suzuki, N. Katada, M. Niwa, *J. Phys. Chem. C* 111 (2007) 894–900.
- [40] B. Hunger, M. Heuchel, L.A. Clark, R.Q. Snurr, *J. Phys. Chem. B* 106 (2002) 3882–3889.
- [41] B. Fubini, V. Bolis, A. Cavenago, P. Ugliengo, *J. Chem. Soc. Faraday Trans.* 88 (1992) 277–290.
- [42] N. Katada, H. Igi, J.H. Kim, M. Niwa, *J. Phys. Chem. B* 101 (1997) 5969–5977.
- [43] I.V. Mishin, T.R. Brueva, G.I. Kapustin, *Adsorption* 11 (2005) 415–424.
- [44] J.S. Kuo, J.W. Rogers, *Surf. Sci.* 453 (2000) 119–129.
- [45] G. Feick, *J. Am. Chem. Soc.* 76 (1954) 5858.
- [46] A. Savara, W.M.H. Sachtler, E. Weitz, unpublished results.
- [47] I. Nova, C. Ciardelli, E. Tronconi, D. Chatterjee, B. Bandl-Konrad, *Catal. Today* 114 (2006) 3–12.
- [48] G.H. Li, C.A. Jones, V.H. Grassian, S.C. Larsen, *J. Catal.* 234 (2005) 401–413.
- [49] J. Szanyi, J.H. Kwak, C.H.F. Peden, *J. Phys. Chem. B* 108 (2004) 3746–3753.
- [50] M.J. Li, Y. Yeom, E. Weitz, W.M.H. Sachtler, *J. Catal.* 235 (2005) 201–208.
- [51] C.C. Addison, *Chem. Rev.* 80 (1980) 21–39.
- [52] R.G. Early, T.M. Lowry, *J. Chem. Soc.* (1922) 963–969.
- [53] J.D.S. Goulden, W.H. Lee, D.J. Millen, *J. Chem. Soc.* (1959) 734–738.
- [54] F.A. Cotton, G. Wilkinson, *Advanced Inorganic Chemistry*, fifth ed., Wiley, New York, 1988, pp. 322–323.
- [55] C. England, W.H. Corcoran, *Ind. Eng. Chem. Fundam.* 13 (1974) 373–384.
- [56] A. Grossale, I. Nova, E. Tronconi, Study of a Zeolite-based system as NH₃-SCR catalyst for Diesel exhaust after treatment, in: NACS 20th North American Meeting, Houston, TX, USA, 2007.
- [57] E. Tronconi, I. Nova, C. Ciardelli, D. Chatterjee, M. Weibel, *J. Catal.* 245 (2007) 1–10.
- [58] M.J. Li, Y.H. Yeom, W.A. Eric, W.M.H. Sachtler, *Catal. Lett.* 112 (2006) 129–132.